Cancer Microenvironment (2018) 11:71–84
https://doi.org/10.1007/s12307-018-0210-8

ORIGINAL ARTICLE

The Influence of Breast Tumour-Derived Factors and Wnt Antagonism on the Transformation of Adipose-Derived Mesenchymal Stem Cells into Tumour-Associated Fibroblasts

Malini Visweswaran[1] · Kevin N. Keane[2] · Frank Arfuso[1] · Rodney J. Dilley[3] · Philip Newsholme[2] · Arun Dharmarajan[1]

Received: 16 October 2017 / Accepted: 28 March 2018 / Published online: 10 April 2018

Abstract

Within the tumour stroma, a heterogeneous population of cell types reciprocally regulates cell proliferation, which considerably affects the progression of the disease. In this study, using tumour conditioned medium (TCM) derived from breast tumour cell lines – MCF7 and MDA MB 231, we have demonstrated the differentiation of adipose-derived mesenchymal stem cells (ADSCs) into tumour-associated fibroblasts (TAFs). Since the Wnt signalling pathway is a key signalling pathway driving breast tumour growth, the effect of the Wnt antagonist secreted frizzled-related protein 4 (sFRP4) was also examined. The response of ADSCs to TCM and sFRP4 treatments was determined by using cell viability assay to determine the changes in ADSC viability, immunofluorescence for mesenchymal markers, glucose uptake assay, and glycolysis stress test using the Seahorse Extracellular Flux analyser to determine the glycolytic activity of ADSCs. ADSCs have been shown to acquire a hyper-proliferative state, significantly increasing their number upon short-term and long-term exposure to TCM. Changes have also been observed in the expression of key mesenchymal markers as well as in the metabolic state of ADSCs. SFRP4 significantly inhibited the differentiation of ADSCs into TAFs by reducing cell growth as well as mesenchymal marker expression (cell line-dependent). However, sFRP4 did not induce further significant changes to the altered metabolic phenotype of ADSCs following TCM exposure. Altogether, this study suggests that the breast tumour milieu may transform ADSCs into a tumour-supportive phenotype, which can be altered by Wnt antagonism, but is independent of metabolic changes.

Keywords Adipose-derived mesenchymal stem cells · Tumour-associated fibroblasts · Tumour conditioned medium · Differentiation · Wnt signalling · sFRP4

✉ Arun Dharmarajan
a.dharmarajan@curtin.edu.au

Malini Visweswaran
malini.visweswaran@postgrad.curtin.edu.au

Kevin N. Keane
kevin.keane@curtin.edu.au

Frank Arfuso
frank.arfuso@curtin.edu.au

Rodney J. Dilley
rodney.dilley@earscience.org.au

Philip Newsholme
Philip.Newsholme@curtin.edu.au

[1] Stem Cell and Cancer Biology Laboratory, School of Pharmacy and Biomedical Sciences, Curtin Health Innovation Research Institute, Curtin University, Perth, WA 6102, Australia

[2] School of Pharmacy and Biomedical Sciences, Curtin Health Innovation Research Institute, Curtin University, Perth, Australia

[3] Ear Sciences Centre, University of Western Australia, Perth, Australia

Introduction

Emerging evidence demonstrates the clinical significance of the surrounding tumour environment in influencing the overall progression of the tumour. The non-neoplastic milieu surrounding a tumour site is composed of diverse non-tumorigenic cellular components such as mesenchymal stem cells (MSCs), macrophages, endothelial cells, epithelial cells, and fibroblasts, which interact with the tumour and enable them to co-evolve and acquire a tumorigenic phenotype [1]. Such transformed cells are termed tumour-associated fibroblasts (TAFs) or cancer-associated fibroblasts, which resemble myofibroblasts and form the foremost cell population within the tumour stroma. These TAFs contribute to the progression and metastasis of the tumour.

However, the exact origin of TAFs remains imprecise, but recent studies indicate that MSCs are one of the major cell populations that the TAFs arise from [2–7]. TAFs are also referred to as "specialised MSCs" to account for their principal cell source. It was reported that when ADSCs were treated

with tumour-derived factors, such as conditioned medium and exosomes derived from the MCF7 and MDA MB2 31 breast cancer cell lines, ADSCs transformed their phenotype into TAFs [2, 3].

There are many signalling pathways that play a role in the transformation of MSCs into TAFs. One of the key pathways regulating the process is the TGFβ1-Smad pathway. In a recent study, the TGFβ1-Smad pathway was upregulated during the transformation of ADSCs into TAFs upon the influence of breast tumour-derived factors [2, 3]. Amongst the other signalling pathways, canonical Wnt signalling has been shown to play a role in sarcomas. A study has reported that activated Wnt signalling promotes transformation of MSCs in sarcomas, while they suggested an opposite mechanism took place in carcinomas [8]. Moreover, the crosstalk between Wnt signalling and TGFβ signalling has been demonstrated where TGFβ increased the accumulation and translocation of β-catenin into the nucleus of various cell types [9–12].

Furthermore, the major canonical Wnt antagonist Dickkopf (Dkk)1 rescued TGFβ-induced skin fibrosis [13], and Wnt antagonists have been demonstrated to inhibit the expression of mesenchymal markers such as vimentin and α-smooth muscle actin, whose expression is heightened in TAFs. Hence, a possible mechanism to disrupt the functionality of TAFs would be to target the heightened proliferative and angiogenic potential of TAFs using Wnt antagonists that also target these properties.

Our Wnt antagonist of interest, secreted frizzled-related protein 4 (sFRP4) has been demonstrated to possess anti-tumorigenic, anti-angiogenic, and pro-apoptotic properties [14–16], and hence would a good candidate to study its potential to curb the process of transformation. Our study is the first to focus on the transformation of ADSCs into TAFs in the presence of sFRP4. We aim to explore the role of sFRP4 in altering various aspects of transformation, such as cell viability, expression of TAF-specific markers, and the metabolic profile of ADSCs. We have chosen ADSCs because they are the resident MSCs within the breast tumour stroma, hence making their potential transformation into TAFs clinically relevant. Moreover, in order to harness the full clinical potential of ADSCs or MSCs for anti-cancer therapies, their capability to transform into a tumorigenic phenotype needs to be fully understood and carefully regulated.

Materials and Methods

Cell Culture

ADSCs were purchased from Lonza, Australia and were cultured in Roswell Park Memorial Institute (RPMI) medium containing 10% foetal bovine serum (FBS) and 1% penicillin-streptomycin (PS). ADSCs at passages P2-P5 were used for the studies. Breast tumour cell lines MCF7 and MDA MB 231 purchased from American Type Culture Collection were cultured in RPMI containing 10% FBS and 1% PS. The cells were incubated in a 5% CO_2 incubator at 37 °C.

Harvest of Tumour Conditioned Medium

For tumour conditioned medium (TCM) harvest, MCF7 and MDA MB 231 cells were cultured up to around 90% confluence in T175 or T75 flasks in RPMI medium containing 10% FBS and 1% PS. For conditioning, the medium was changed to serum-free RPMI containing 1% PS, and the conditioning was performed for 24 h. 25 mL of fresh serum-free RPMI containing 1% PS was added to a T175 flask, or 10 mL of the same was added to a T75 flask for conditioning. After 24 h, the TCM was harvested and centrifuged at 2000 g for 10 min, and filtered through 0.22 μm syringe filters to perform treatments on ADSCs. The treatments with TCM were performed on ADSCs for both 4 days and 10 days, so as to observe the effects of TCM for a relatively shorter and longer duration.

Morphological Observation for Treatments

ADSCs were observed for morphological changes and micrographs captured at the end-point of indicated treatment durations. As a positive control for myofibroblast differentiation, TGF-β was used at different doses – 0.2, 2, 5, and 10 ng/mL, Lysophosphatidic acid (LPA) was used at 5 and 10 μM concentration for treating ADSCs for 10 days. Further, in order to confirm that the TGF-β-induced differentiation could be rescued, a pharmacological inhibitor of TGF-β receptor signalling - SB431542 was used at 10 μM for 4 days.

Cell Viability

ADSCs were seeded at 2500 cells/well in a 96-well plate and allowed to adhere onto the tissue culture-treated surface overnight. The next day, the medium was removed and the treatment wells were replaced with 100 μL MCF7 TCM and MDA MB 231 TCM for short-term (4 days) and long-term (10 days) studies. In control wells, the medium was removed and replaced with 100 μL serum-free RPMI containing 1% PS. In specific treatment wells, simultaneous exogenous addition of sFRP4 was performed at 250 pg/mL concentration (as this concentration was optimised in our laboratory in previous studies [15, 17, 18]), along with TCM. On day 4 or day 10, 10 μL of 5 mg/mL MTT (Sigma) was added to each well containing 100 μL medium and left for 4 h at 37 °C. After 4 h, the medium was removed from all the wells and the resulting formazan crystals were dissolved in 100 μL

DMSO. The absorbance was measured using a plate reader (Enspire multimode, Perkin Elmer) at 595 nm.

Immunofluorescence

ADSCs were seeded at 2500 cells/well in a 96-well plate and allowed to adhere onto the tissue culture-treated surface overnight. The next day, the medium in treatment wells was replaced with TCM derived from MCF7 and MDA MB 231 for 10 days. The medium in control wells was replaced with serum-free RPMI containing 1% PS. In specific treatment wells, simultaneous exogenous addition of sFRP4 was performed at 250 pg/mL concentration. On day 10, the medium was removed from all wells and the cells were rinsed with PBS twice. The cells were fixed with 4% paraformaldehyde for 20 min and were rinsed with PBS twice. Following fixation, the cells were permeabilised with 0.3% saponin for 2–5 min, and rinsed with PBS, then incubated in blocking solution containing 0.5% bovine serum albumin, 0.3% saponin, and 1% normal goat serum for 1 h at room temperature, and then rinsed with PBS. After blocking, the cells were incubated in primary antibody (α-smooth muscle actin and vimentin, Cell Signaling Technology) at 1:200 dilution prepared in blocking buffer. The primary antibody incubation was performed overnight at 4 °C. The next day, the primary antibody solution was removed and followed by 2 PBS rinses to all wells. The secondary antibody solution at 1:200 dilution was prepared in blocking solution, added to all wells, and left to incubate for 1 h at room temperature. Following this, the cells were rinsed in PBS and 4′,6-diamidino-2-phenylindole, dihydrochloride (DAPI) at 1:10000 dilution was added to all the wells for 5 min. The DAPI was removed, cells were rinsed with PBS, and viewed under an inverted confocal microscope (Nikon). The images were captured at the same microscopic settings and exported to TIFF format using Nikon NIS-elements software, and the fluorescence intensity of the whole micrographs was measured from a minimum of 5 images/treatment using Image J software, and the intensity was compared relative to untreated control.

Glucose Uptake Assay

Glucose uptake by the ADSCs was measured using the luminescence-based glucose uptake glo-assay kit (Promega). ADSCs were seeded at 1000 cells/well in a white 96 well plate and allowed to attach to the tissue culture surface. After that, cells were exposed to 100 μL MCF7 TCM and MDA MB 231 TCM ± 250 pg/mL sFRP4 for 4 days. After 4 days of treatment, the medium was removed slowly and the cells were washed gently with PBS twice to remove any residual glucose from the medium. After the PBS wash, 50 μL of 2-deoxyglucose (2-DG) was added at 1 mM and incubated for 10 min at 37 °C. 1 mM 2-DG was freshly prepared in PBS from the 100 mM 2-DG stock provided in the kit. 2-DG is a glucose analogue that is transported across the cell membrane similar to glucose and is phosphorylated into 2-DG-6-phosphate (2DG6P). Once the 2DG6P accumulated inside the cell, the reaction was stopped after 10 min of incubation by adding 25 μL stop buffer, which lyses the cells and stops the reaction. 25 μL of neutralisation buffer was added to neutralise the acid and this was followed by addition of 100 μL of 2DG6P detection reagent. The detection reagent consists of glucose-6-phosphate dehydrogenase (G6PDH), $NaDP^+$, reductase, ultra-glo recombinant luciferase, and proluciferin substrate, and was prepared at least 1 h before addition to allow it to equilibrate to room temperature. Following addition of the detection reagent, the cells were incubated at room temperature for 30 min up to 6 h, and the luminescence was recorded using a plate reader (Enspire multimode, Perkin Elmer). The luminescence corresponds to the concentration of 2DG6P, which correlates to the amount of glucose taken up by the cells.

Seahorse Extracellular Flux Analysis

Potential alterations in metabolic flux following transformation from ADSCs into TAFs was assessed using Seahorse XF^e96 flux analyser (Agilent Technologies) and a standard glycolysis stress test (Agilent Technologies), which allows the determination of the glycolytic rate, glycolytic capacity, and glycolytic reserve (Table 1). A change in the metabolic phenotype of ADSCs switching from oxidative phosphorylation to glycolysis was assessed after treating the ADSCs with TCM from MCF7 and MDA MB 231 tumour cell lines.

ADSCs were seeded at 3000 cells/well in a 96 well plate (Agilent Technologies) specifically designed for Seahorse analysis in RPMI medium containing 10% FBS and 1% PS. After ADSCs attached to the plate surface, the medium was replaced with MCF7 TCM and MDA MB 231 TCM in treatment groups. ADSCs growing in serum-free RPMI were used as a control. 250 pg/mL sFRP4 was added to the TCM-containing wells and wells containing non-conditioned control medium. The treatments were performed for 10 days.

On the day before the assay, the Seahorse cartridge containing the sensor probes was immersed in 200 μL calibration solution/well and incubated in a non-CO_2 incubator at 37 °C for hydration. Glucose-free DMEM was prepared for the assay using Dulbecco's modified Eagle's medium (DMEM) powder (Sigma) dissolved and made up to 1 L using milliQ water. 2 mM glutamine, 1 mM sodium pyruvate, and phenol red were added to the medium, and the pH was adjusted to 7.35 ± 0.05 using freshly prepared 1 M NaOH. The medium was filtered using a bottle-top filter (Thermo Scientific) and stored at 4 °C.

On the day of the assay, the medium in the wells was gently removed and 3 medium changes were performed manually

Table 1 Metabolic parameters measured using glycolysis stress test with Seahorse XF^{e}96 flux analyser

Metabolic parameter	Significance	Equation
Glycolytic rate	Provides the rate of glycolysis (conversion of glucose to pyruvate) under basal conditions. It is obtained by measuring ECAR after addition of saturating concentration of glucose.	Maximum ECAR measurement before oligomycin injection – Last rate measurement before glucose injection
Glycolytic capacity	Provides the maximum glycolytic capacity by measuring ECAR following addition of oligomycin (an ATP synthase inhibitor), which shifts the energy production to glycolysis.	Maximum ECAR measurement after oligomycin injection – Last measurement before glucose injection
Glycolytic reserve	Measures the difference between the maximum glycolytic capacity and glycolytic rate at basal conditions. It indicates the ability of the cell to respond during lack of energy production through oxidative phosphorylation.	Glycolytic capacity – Glycolytic rate
Non-glycolytic acidification	Measures the ECAR after addition of 2-DG, Indicates ECAR caused by cell processes other than glycolysis.	Minimum ECAR measurement after addition of 2-DG

using the prepared glucose-free medium. The final medium volume per well was 175 μL and was incubated at 37 °C in the non-CO_2 incubator for at least 1 h. The assay was performed through injection of 3 metabolic compounds - glucose, oligomycin, and 2-DG. Injection of glucose facilitates exposure to a saturating concentration of glucose at 25 mM. The second injection facilitates the exposure to oligomycin at 1 μM, which inhibits ATP synthase and minimises ATP production from oxidative phosphorylation. The third injection facilitates the exposure to 2-DG at 100 mM, which blocks glycolysis. All injection volumes were maintained at equal volumes of 25 μL.

The metabolic parameters measured are listed in Table 1.

The 4 parameters measured using the Seahorse flux analyser, the significance for measurement, and the formulae for performing the calculations are indicated.

Statistical Analysis

Experiments (cell viability, glucose uptake assay, seahorse flux analysis) were performed in at least 3 biological replicates. For immunofluorescence, at least 5 images were captured per treatment group. The mean values ± SEM were determined and the statistical significance was calculated using One-way ANOVA and Student's t-test to compare between the values of treatment conditions against untreated controls (indicated by *) and between treatment groups (indicated by #). A p value of <0.05 was considered to be statistically significant. The graphs were prepared using GraphPad Prism software, and the images were prepared using Microsoft PowerPoint software, and the resolution was increased using Adobe Photoshop CS6.

Data Availability The data supporting the results of this manuscript are included within the article.

Results

Morphological Changes in ADSCs during Transformation

ADSCs were treated with TCM derived from MCF7 and MDA MB 231 tumour cell lines for 10 days. Different doses of TGF-β and LPA were used on ADSCs for 10 days as positive controls for myofibroblastic differentiation. The cells were regularly observed for morphological changes during the treatment conditions, and micrographs captured of all treatment groups on day 10 of treatment (Fig. 1). The control ADSCs in Fig. 1a show a change from the normal spindle-shaped morphology of ADSCs; the cells appear more rounded due to the serum-free culture conditions. This does not occur in TCM-treated ADSCs although the TCM is serum-free. As compared to control, the TCM-treated ADSCs show a distinct change into a spindle-like morphology with the appearance of cytoplasmic stress fibres, indicating a shift towards a myofibroblastic nature (Fig. 1a). Fig. 1b shows the myofibroblastic differentiation of ADSCs in the presence of recombinant TGF-β protein (as a positive control for myofibroblastic differentiation) at doses of 0.2 ng/mL, 2 ng/mL, 5 ng/mL, and 10 ng/mL.

Further, the pharmacological inhibitor SB431542, which inhibits TGF-β receptor signalling, was used in combination with 2 ng/mL TGF-β for 4 days. While 2 ng/mL TGF-β treatment alone showed a morphological change indicative of 'myofibroblastic' differentiation, the combination treatment prevented the morphological change of ADSCs (Fig. 1c). This showed that the transformation of ADSCs could be rescued by inhibiting TGF-β signalling. Additionally, LPA was also used at 5 μM and 10 μM doses to induce myofibroblastic differentiation of ADSCs (Fig. 1d).

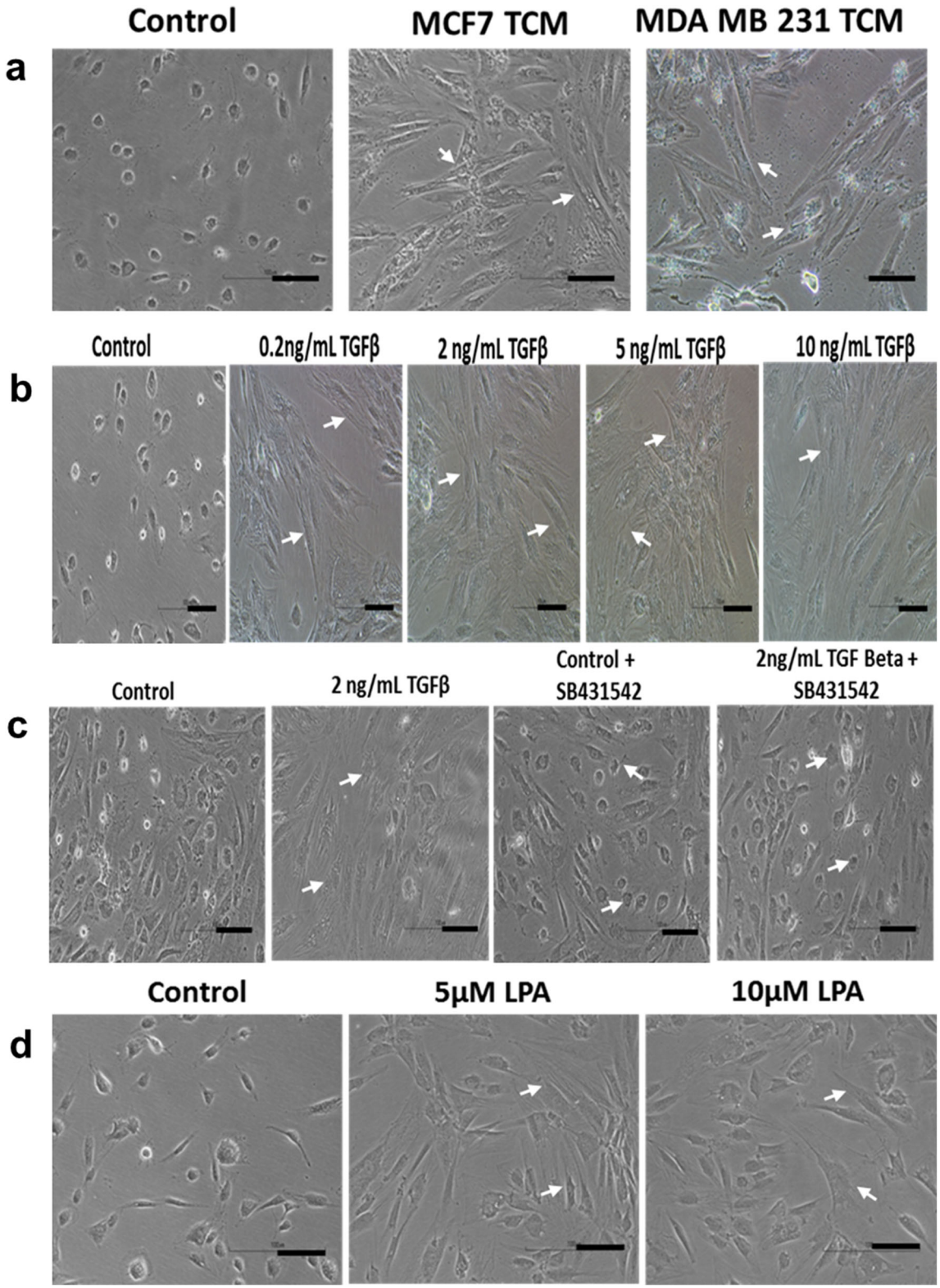

Fig. 1 Morphology of ADSCs during transformation into TAFs. ADSCs were treated with **a** TCM derived from MCF7 and MDA MB 231 tumour cell lines, **b** recombinant TGF-β at different doses, **c** recombinant TGF-β in the presence of TGF-β receptor inhibitor SB431542 (as negative control), **d** different doses of LPA. Arrows indicate the difference in morphological features of ADSCs upon treatment with TCM, TGF-β, and LPA. Scale bar = 100 μM

Cell Viability

We found that TCM from MCF7 and MDA MB 231 cells increased the viability of ADSCs after short-term (Day 4) (Fig. 2a, c) and long-term treatment (Day 10) (Fig. 2b, d). MCF7 TCM increased the viability to almost 1.95-fold, whereas sFRP4 co-treatment decreased this to 1.46-fold (Fig. 2a). Similarly, MDA MB 231 TCM increased viability to 1.81-fold whereas, in the simultaneous presence of sFRP4, the viability was reduced to 1.49-fold at 4 days (Fig. 2c). After 10 days of MCF7 TCM treatment, the viability of ADSCs increased to 2.42-fold, whereas in the presence of sFRP4 the TCM-induced viability was reduced to 1.82-fold (Fig. 2b). Likewise, MDA MB 231 TCM increased the viability to 1.73-fold, whereas co-treatment with sFRP4 reduced the TCM-induced viability to 1.23-fold (Fig. 2d). As compared to the effect of sFRP4 on viability reduction of control ADSCs, a ~2-fold greater reduction was observed with the effect of sFRP4 on the viability of TCM-treated ADSCs. We also performed cell viability assays with various TGF-β doses at 2, 5, and 10 ng/mL, which resulted in an increase in cell viability of ADSCs, followed by a reduction with the combination treatment of TGF-β and its inhibitor SB431542, after both 4-day and 10-day treatments (data not shown).

The rise in cell viability is one of the characteristic features that indicate the transformation of ADSCs into a tumour-supportive phenotype. The supplementation of sFRP4 decreased the TCM-induced increase in the cell viability of ADSCs, suggesting that sFRP4 downregulates the transformation of ADSCs into TAFs.

Expression of TAF-Associated Mesenchymal Markers

We found that TCM from MCF7 and MDA MB 231 cells upregulated the expression of TAF-associated markers in ADSCs. Using immunocytochemistry, we demonstrated that MCF7 TCM upregulated the fluorescence signal for α-smooth muscle actin (α-SMA) and vimentin after 10 days of treatment in ADSCs (Fig. 3). However, sFRP4 inhibited the MCF7 TCM-induced increase in the signal, thereby indicating a reduced transformation (Fig. 3a, b). (Fig. 3c, d). The fluorescence intensity of α-SMA increased to 3.94-fold with MCF7 TCM, which was reduced to 2.73-fold in the presence of sFRP4 (Fig. 3a, c). The fluorescence intensity of vimentin was increased to 10.54-fold, which was reduced to 5.6-fold in the presence of sFRP4, thereby indicating reduced transformation (Fig. 3b, d).

It was also found that the TCM derived from the MDA MB 231 cell line upregulated the transformation into TAFs by increasing the expression of α-SMA and vimentin (Fig. 4b). However, no difference was observed between MDA MB 231 TCM alone and MDA MB 231 TCM + sFRP4 in terms of α-SMA expression (Fig. 4a, c). The fluorescence intensity of vimentin was increased to 2.60-fold when treated with MDA MB 231 TCM alone, which was reduced to 2.22-fold in the presence of sFRP4 (Fig. 4b, d).

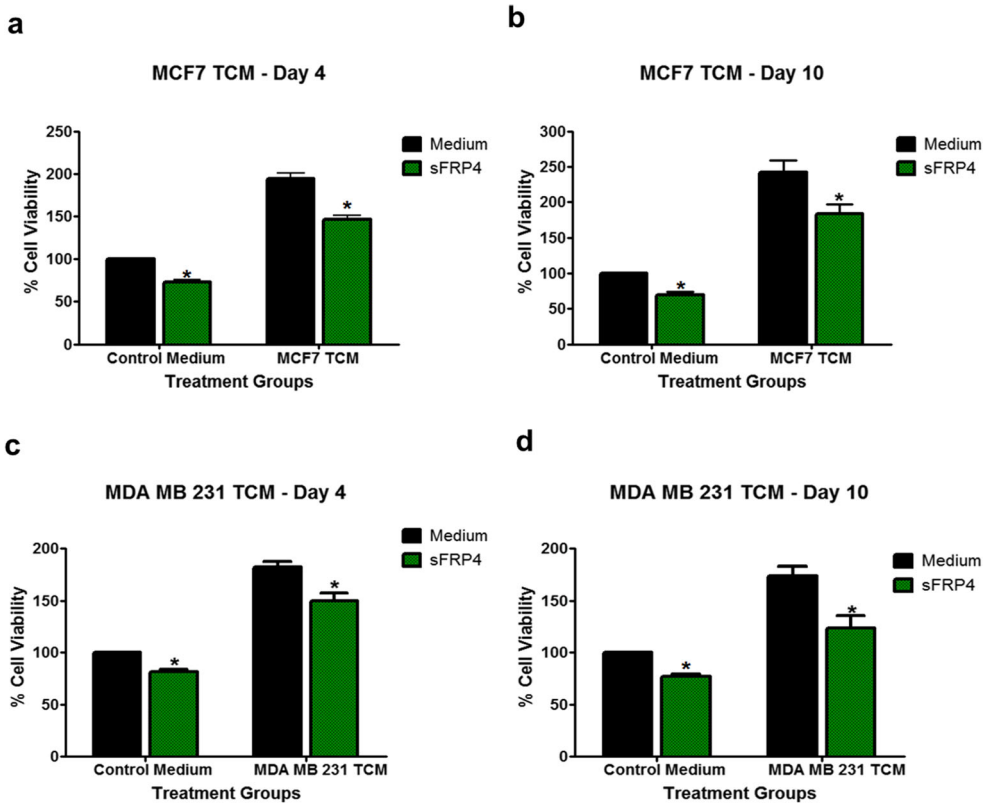

Fig. 2 Cell viability of ADSCs during transformation into TAFs. ADSCs were treated with TCM derived from MCF7 and MDA MB 231 tumour cell lines ±250 pg/mL sFRP4 for the indicated time durations. ADSCs treated with MCF7 TCM and sFRP4 at **a** Day 4, **b** Day 10. ADSCs treated with MDA MB 231 TCM and sFRP4 at **c** Day 4, and **d** Day 10

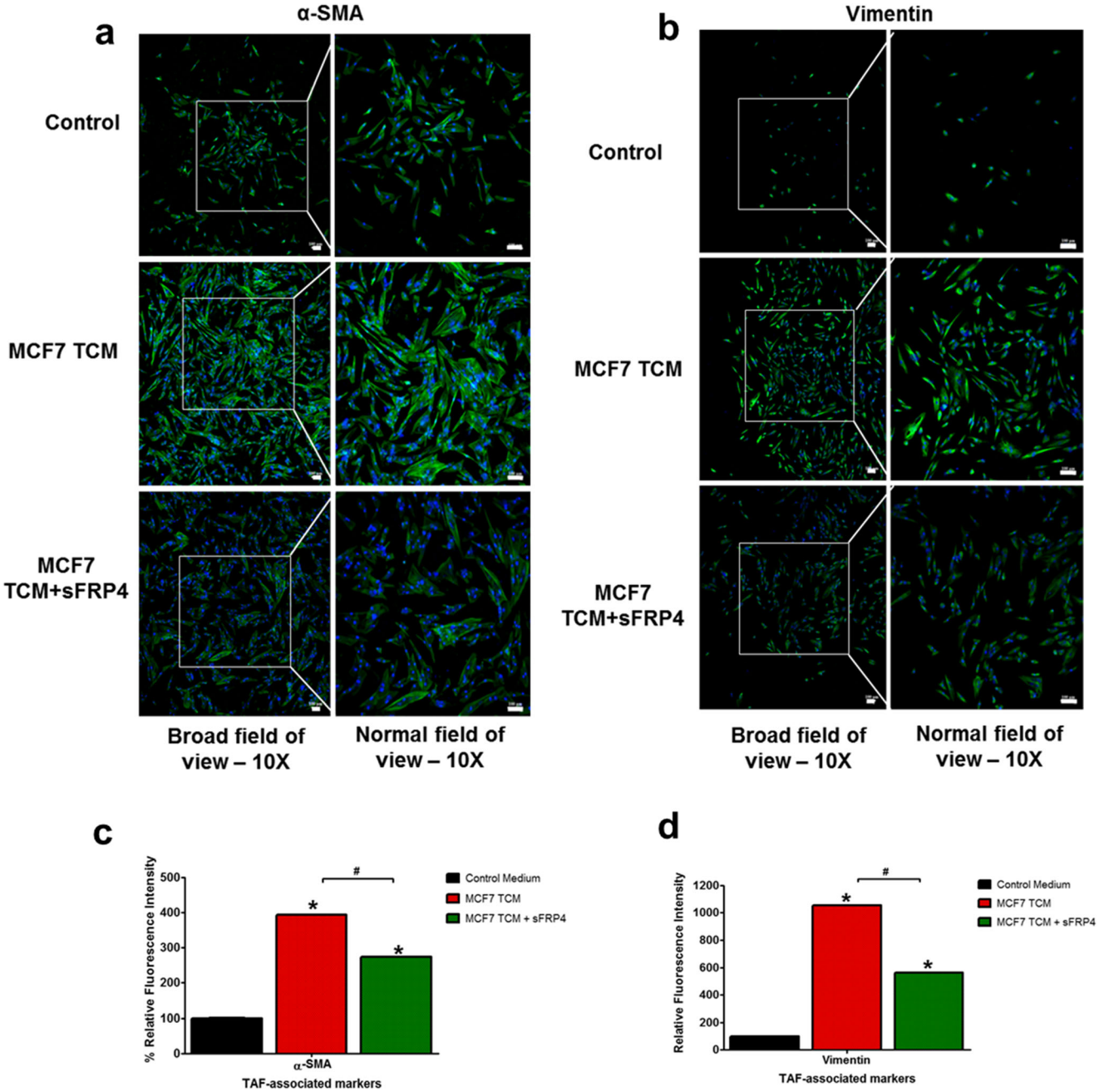

Fig. 3 Confocal immunofluorescent imaging of ADSCs in the presence of MCF7 TCM. ADSCs treated with MCF7 TCM ± 250 pg/mL sFRP4 at Day 10. Expression of **a** α-SMA, **b** vimentin. Left panel of each image shows a broad field of view captured using 10X objective and the right panel shows a normal field of view captured using 10X objective of a Nikon confocal microscope. **c** and **d** show quantitative measurement of fluorescent intensity of α-SMA and vimentin respectively, measured using the captured immunofluorescent images and analysed using Image J software

Glucose Uptake Assay

ADSCs were treated with TCM treatments from MCF7 and MDA MB 231 cells supplemented with and without sFRP4 for 4 days. It was observed that the treatments increased the glucose uptake potential of ADSCs. However, there was no difference in the glucose uptake rates when sFRP4 was added to the TCM treatments (Fig. 5a, b).

Metabolic Flux Determination of TAFs Using Seahorse Flux Analyser – Glycolysis Stress Test

The glycolytic profile of ADSCs during the glycolytic stress test following treatments with MCF7 TCM and MDA MB 231 TCM is shown in Fig. 6a, f. It was observed that on Day 10 of the treatment, TCM from MCF7 and MDA MB 231 stimulated the glycolytic rate (Fig. 6b, g) and decreased the glycolytic

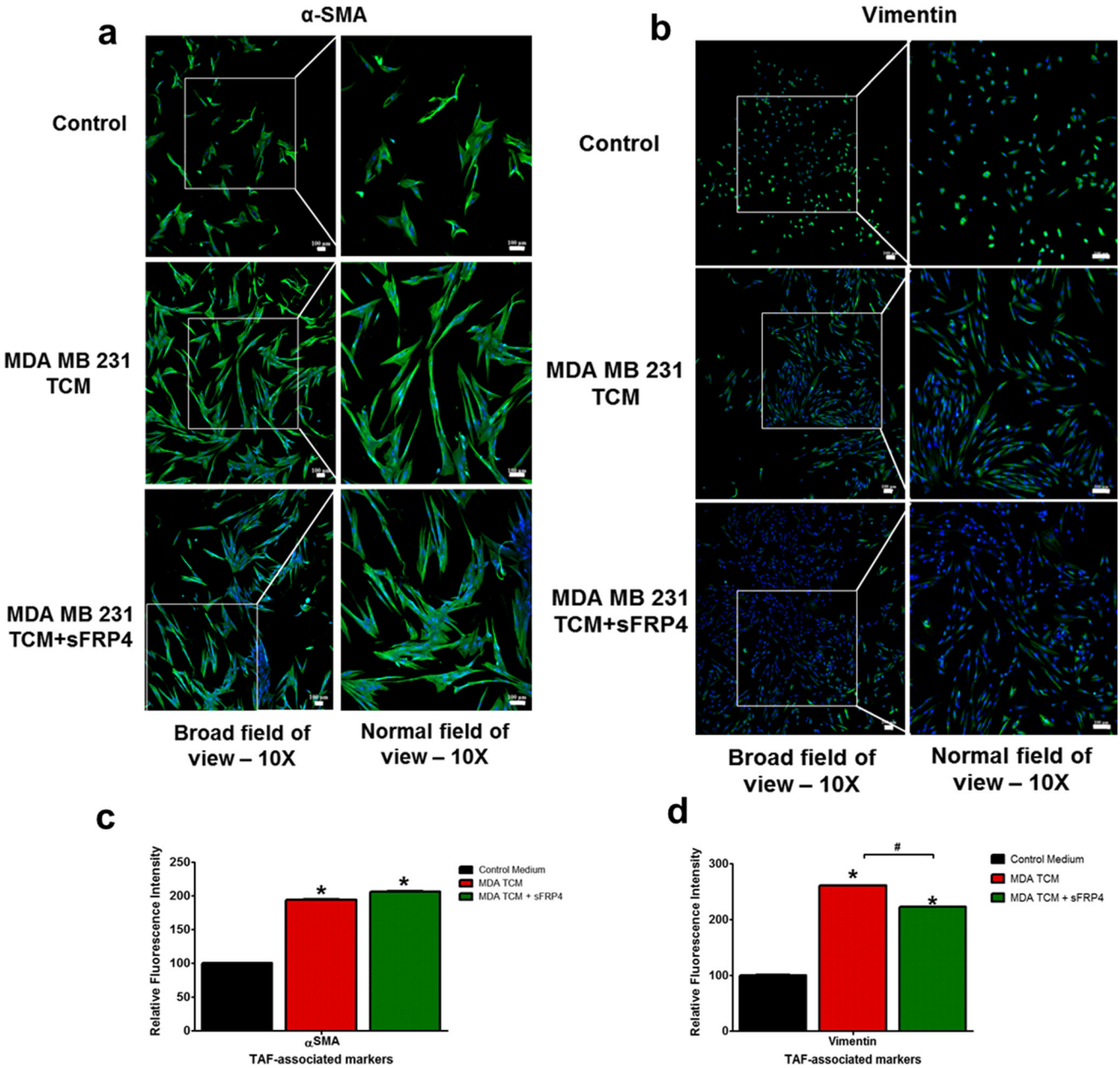

Fig. 4 Confocal immunofluorescent imaging of ADSCs in the presence of MDA MB 231 TCM. ADSCs treated with MDA MB 231 TCM ± 250 pg/mL sFRP4 at Day 10. Expression of **a** α-SMA, **b** vimentin. Left panel of each image shows a broad field of view captured using 10X objective and the right panel shows a normal field of view captured using 10X objective of a Nikon confocal microscope. **c** and **d** show quantitative measurement of fluorescent intensity of α-SMA and vimentin respectively, measured using the captured immunofluorescent images and analysed using Image J software

reserve of ADSCs (Fig. 6d, i). The increase in glycolytic rates indicated the transformation of the metabolic phenotype of ADSCs into a glycolytic profile, but no differences were observed when the MCF7 TCM or MDA MB 231 TCM was supplemented with sFRP4 (Fig. 6b, g). No significant differences were observed in the glycolytic capacity and non-glycolytic ECAR in response to MCF7 TCM treatments (Fig. 6c, e, h, j).

The oxygen consumption rates (OCR) were also measured after the 10-day treatments. The OCR, which reflects oxidative phosphorylation was almost undetectable (data not shown), which indicated the significant reliance of ADSCs on glycolytic metabolism. However, when stimulated with glucose, the TCM-treated cells increased their ECAR faster and to a greater extent in comparison with the control ADSCs.

Discussion

Non-tumour cells in close proximity to the tumour have been shown to be the origin of TAFs, which attain a pro-

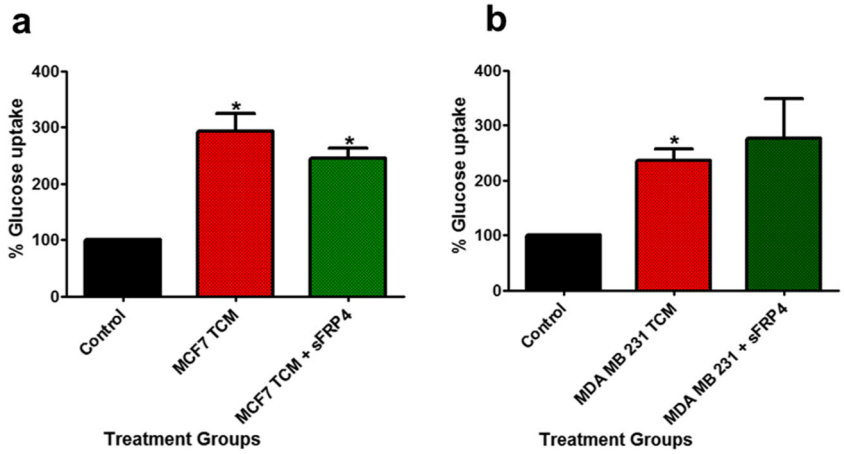

Fig. 5 Glucose uptake rates of ADSCs during transformation into TAFs. ADSCs were treated with **a** TCM derived from MCF7 ± 250 pg/mL sFRP4, and **b** TCM derived from MDA MB 231 ± 250 pg/mL sFRP4 for 4 days

tumorigenic and aggressive phenotype, and have been shown to promote cancer progression. Earlier studies have reported the pro-tumorigenic properties of TAFs, as they are a rich source of pro-tumorigenic and pro-angiogenic molecules

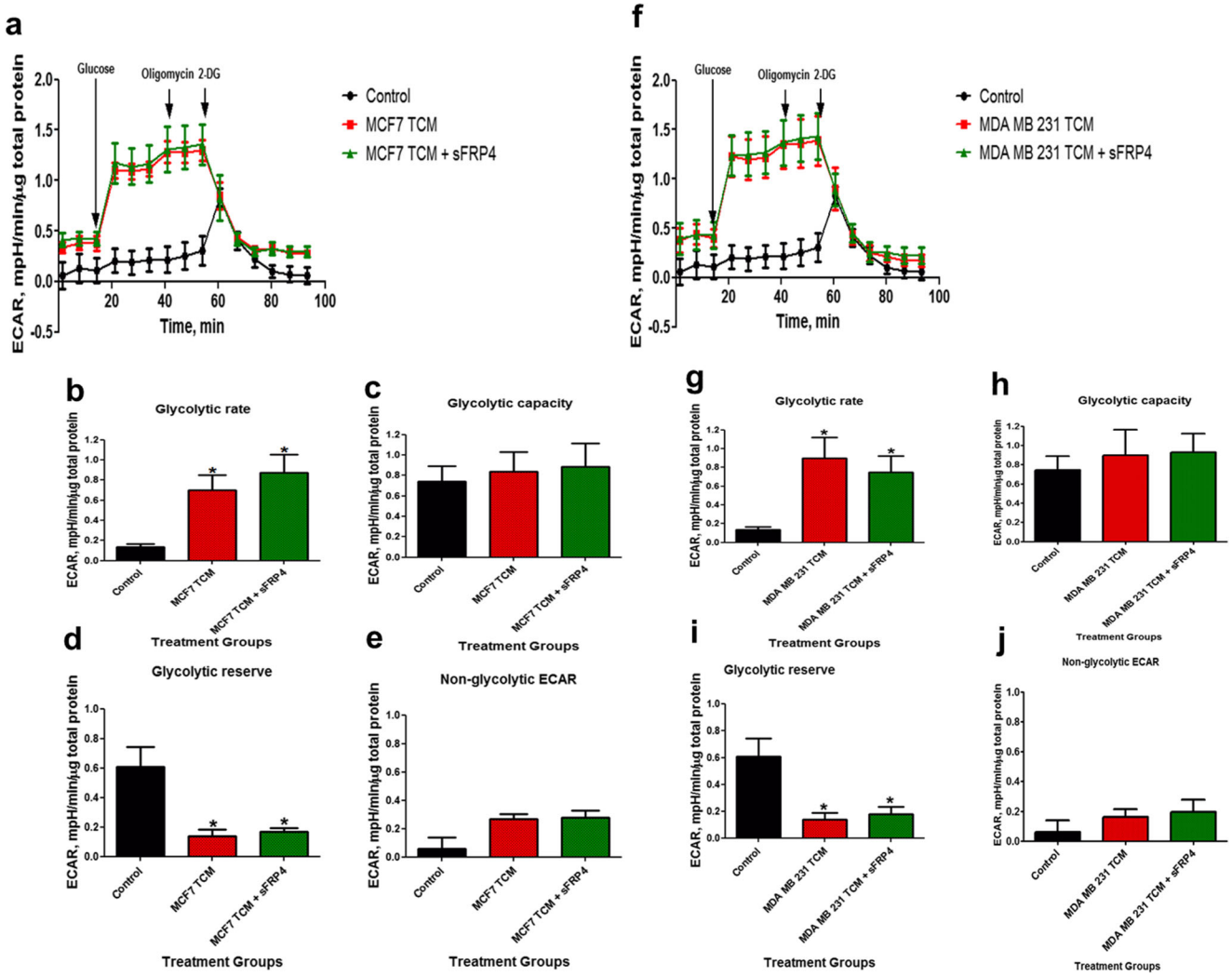

Fig. 6 Metabolic profile of ADSCs during transformation into TAFs. ADSCs were treated with MCF7 TCM ± 250 pg/mL sFRP4 and MDA MB 231 TCM ± 250 pg/mL sFRP4 for 10 days. Glycolytic profile of ADSCs during glycolysis stress test by measuring the ECAR using the Seahorse Flux Bioanalyser following **a** MCF7 TCM, and **f** MDA MB 231 TCM treatments. **b**-**e**, and **g**-**j** are the glycolytic rates, glycolytic capacity, glycolytic reserve, and non-glycolytic ECAR following MCF7 TCM and MDA MB 231 TCM treatments respectively

[19, 20]. TAFs have been recognised as a crucial constituent of the tumour stroma and have been reported to promote tumour development in a variety of different ways, such as cancer growth, invasion, metastasis, therapeutic resistance, angiogenesis, extracellular matrix remodelling, and metabolic reprogramming [21]. In terms of their tumour-promoting property, one study reported upregulated viability in tumour cells when treated with conditioned medium from TAFs [22]. Another study showed that hepatocyte growth factor secreted from TAFs enhanced breast tumour colony formation in MDA MB 468 and SKBR3 breast cancer cells [23]. Conditioned medium from oral squamous cell carcinoma cells has been shown to transform stromal fibroblasts into myofibroblasts, which further contributed to tumour development. The transdifferentiation observed in these studies was attributed to the secretion of TGF-β1 by the tumour cells [24, 25]. In another study, the LPA present in A549 lung cancer cell CM was shown to be responsible for inducing the differentiation of ADSCs into TAFs, which was abrogated when the LPA receptor was silenced or when ADSCs were treated with the LPA inhibitor Ki16425 [26].

Our study demonstrated a change in the morphology of ADSCs as they were exposed to TCM treatments. Even though the TCM was serum-free, the ADSCs displayed strong attachment to the culture surface, spindle-like shape, and accumulation of cytoplasmic stress fibres within the cells, which are characteristic feature of myofibroblastic differentiation [27]. Stress fibres are bundles of actin filaments that are needle-shaped and involved in contractile activity of cells [28]. The treatment of ADSCs using TGF-β and LPA, which are known inducers of myofibroblast differentiation [2, 29–31], induced similar morphological changes and confirmed the transformation of ADSCs into a myofibroblast phenotype. Further, treatment with the TGF-β receptor inhibitor - SB431542 confirmed that the myofibroblastic transformation of ADSCs was preventable via inhibition of signal transduction pathways [2].

There was an increase in the viability of ADSCs as they underwent transformation in the presence of MCF7 TCM and MDA MB 231 TCM. Indicative of their attainment of the TAF phenotype, earlier studies have demonstrated that MSCs isolated from tumour sites exhibited greater proliferative capacity than naïve MSCs, such as the MSCs isolated from ovarian, pulmonary [32], gastric [33], and prostate cancers [34]. This could be attributed to the presence of proliferation-related genes such as MDM2, p21, and zinc finger transcriptional factor sal-like protein 4 [35]. However, these differences had been delineated between normal MSCs and the MSCs isolated from the tumour site. No previous studies have shown the increase in viability of MSCs during their transformation into TAFs in the presence of TCM derived from MCF7 and MDA MB 231 cells during the transformation process at short-term (Day 4) and long-term (Day 10) time-points. This is indicative of their supportive role in tumour growth. It also validates that MSCs are one of the precursor populations for TAFs. Moreover, TCM was capable of ameliorating the effects induced by serum deprivation of ADSCs. However, it needs to be noted that the increase in cell viability of ADSCs following MDA MB 231 TCM treatments was similar after Day-4 and Day-10, which suggests the maximum proliferative capacity of these cells had been attained under these limiting conditions, such as the absence of serum in the TCM treatments.

Further to the promoting activity of TCM, this study is the first to demonstrate the role of the Wnt inhibitor sFRP4 in reversing this transdifferentiation. The presence of sFRP4 reduced the TCM-induced increase in MSC viability at both the short (Day 4) and long (Day 10) term treatments. This could be attributed to the anti-tumorigenic and pro-apoptotic property of sFRP4 reported earlier in various cell lines [14, 16, 18, 36, 37].

MSCs transforming into TAFs under the influence of tumour-derived factors have been demonstrated to have higher expression of mesenchymal markers [2, 6]. Similarly, our immunofluorescence results demonstrated higher expression levels of α-SMA and vimentin when MSCs were treated in the presence of TCM derived from MCF7 and MDA MB 231 cells. Assimilation of α-SMA in the stress fibres within the cell is one of the characteristics of myofibroblast differentiation, providing the cells with a higher contractile activity [38, 39]. Further, we demonstrated that when sFRP4 was delivered simultaneously with TCM, there was a reduction in the TCM-mediated increase in these marker expressions. This could be correlated to the reduction in mesenchymal-specific markers due to sFRP4 observed in various other cell lines [40, 41]. However, when sFRP4 was added to MDA MB 231 TCM, there was a decrease observed in only vimentin expression. Therefore, it indicates that sFRP4 is effective in targeting another aspect of ADSCs transforming into TAFs by modulating the mesenchymal-defining markers, although it depends on the type of stimuli involved in the transformation. However, the differences in the cell size, area, and viability of ADSCs in response to these treatments should also be taken into account when interpreting the fluorescence levels.

Further, in order to investigate any metabolic transformation of ADSCs into TAFs, a glucose uptake assay was performed. It was observed that after 4 days of undergoing TCM treatment, the ADSCs upregulated their glucose uptake rates. According to the 'Warburg effect' [42], a higher glucose uptake is observed in cancer cells during aerobic glycolysis. These results suggest that the tumour microenvironment was successful in reprogramming the normal metabolic functions of ADSCs, forcing the ADSCs to bear a highly glycolytic phenotype with higher glucose uptake. This would permit higher production of lactate and other energy-rich metabolic intermediates such as pyruvate, which could be utilised by the

tumour cells to provide precursors for macromolecules essential for their growth. However, the potential differences that occur in cell viability with the treatments also need to be accounted for.

Next, the glycolytic activity was assessed using Seahorse flux analysis. It was found that when ADSCs were treated with TCM from MCF7 and MDA MB 231 cells, there was an upregulation in their basal glycolytic rates. This suggests that, when exposed to TCM, the ADSCs are more glycolytically driven than the control ADSCs, and echoes the results for the glucose uptake assay above. The control ADSCs appeared glycolytically inactive, with a delayed increase in their ECAR only after 60 min following the initiation of the glycolysis stress test. During this lag phase, whether the control ADSCs opted for mitochondrial respiration for their energy production was also determined by measuring their OCR. It was found that the control ADSCs did not increase their OCR, indicating that the control ADSCs chose to remain metabolically dormant (data not shown). Following this metabolically dormant phase, control ADSCs exhibited a late increase in their ECAR at 60 min after the addition of oligomycin, (an ATP synthase inhibitor), which shuts off mitochondrial oxidative phosphorylation and drives cells to use glycolysis to their maximal capacity. Therefore, it appears that the control ADSCs responded by a switch to glycolytic activity only after they were forced to do so, and this resulted in a late increase in their ECAR. On the other hand, ADSCs treated with TCM responded immediately to glycolytic stimulation, with a rapid and large increase in ECAR following exposure to glucose, and thereafter with oligomycin, indicating that the metabolic capability of the conditioned cells remained greater.

However, the control ADSCs and TCM-treated ADSCs exhibited no significant difference in their glycolytic capacity. This could be due to the delayed ECAR increase observed in control ADSCs resulting in generating a higher glycolytic capacity, which was almost similar to the glycolytic capacity of TCM-treated ADSCs. The next parameter measured was the glycolytic reserve, which is the difference between glycolytic rates and glycolytic capacity. Although the control ADSCs exhibited low glycolysis rates, their late increase in ECAR resulted in a glycolytic capacity similar to the TCM-treated ADSCs, resulting in a higher glycolytic reserve measure. On the other hand, the TCM-treated ADSCs displayed higher glycolytic rates followed by a similar glycolytic capacity as compared to the control ADSCs, resulting in a reduced glycolytic reserve measure.

Hence, it needs to be noted from these results that even though the conditions were serum-free, TCM-treated ADSCs appeared to be more metabolically-responsive and glycolytically-driven as compared to the control ADSCs. The tumour-derived factors present in the TCM protected the ADSCs from reverting into a metabolically dormant state. Overall, the findings from the Seahorse flux analysis could be also linked to the increased glucose uptake by the ADSCs when treated with TCM for 4 days as compared to the control ADSCs, observed using the glucose uptake assay. This also correlates with earlier studies indicating the metabolic transition towards aerobic glycolysis in TAFs, attributed to the 'reverse Warburg effect' induced by the tumour environment on the surrounding non-tumour cells, resulting in the production of energy-rich metabolic intermediates that are in turn used by tumour cells for their growth [43, 44]. However, sFRP4 did not further affect the metabolic activity of TCM-treated ADSCs, with no changes in their glucose uptake rates, glycolytic rates, glycolytic activity, and glycolytic reserve. Our findings are similar to a previous study that reported no change in metabolic parameters such as ATP turnover, glucose utilisation, basal OCR, maximum respiration, and spare respiration capacity in JU77 mesothelioma cells in response to sFRP4 treatment [18].

So far, TGF-β signalling has been found to be a key pathway in promoting transformation of MSCs into myofibroblasts and has been shown to be involved in their metabolic reprogramming towards increased glycolysis [45]. Another study has delineated the mechanism underlying the metabolic transition, where it was demonstrated that a downregulation of isocitrate dehydrogenase-3α enzyme occurred, which further reduced α-ketoglutarate, leading to destabilisation of hypoxia inducible factor-1α and thereby upregulation of glycolysis [46].

In previous studies it has been shown that sFRP4 inhibits mesenchymal marker and β-catenin expression by targeting the Wnt signalling pathway [47]. However, no studies so far have shown the presence of Wnt being secreted in the TCM, which needs to be further investigated. Nevertheless, it is known that the tumour cells secrete various growth factors into their conditioned medium that may influence several signalling pathways. One of the previous studies on TCM derived from breast cancer cells reported the presence of secreted TGF-β1 in TCM. In the study, both MDA MB 231 and MCF7 cells have been shown to secrete a significant amount of TGFβ1 into the medium after 24 h and 48 h conditioning duration [2]. Further, inhibition of TGFβ1 signalling reduces mesenchymal marker expression in ADSCs [2]. In addition, it has already been demonstrated by several studies that TGFβ signalling crosstalks with the Wnt signalling pathway. TGFβ has been shown to cause an increased accumulation and translocation of β-catenin into the nucleus of various cell types, indicating that both the TGFβ and the Wnt signalling pathways possess the ability to crosstalk with each other [9–12]. Moreover, another study showed that the canonical Wnt antagonist Dickkopf-1 rescued TGFβ-induced skin fibrosis [13]. Hence, in accordance with the established findings, we assume that sFRP4 may be blocking the TCM activity either

through the Wnt signalling pathway or through establishing crosstalk with other signalling pathways such as the TGFβ-driven pathway.

Overall, this study has demonstrated the role of ADSCs in their possible transformation towards a pro-tumorigenic phenotype and their partial regulation by sFRP4. Factors from the TCM exerted a protective effect on ADSCs by preventing their reversion into a morphologically, functionally, and metabolically less active state, as seen in control ADSCs. Although being serum-free, the TCM applied a promoting activity on ADSCs by increasing their viability rates and mesenchymal marker expression, and making the cells more glycolytic. The Wnt antagonist sFRP4 controlled the transformation of ADSCs by reducing the viability and marker expressions induced by the TCM. However, sFRP4 had no role in regulating the metabolic switch driving the ADSCs towards a glycolytic phenotype upon exposure to TCM. This study becomes clinically important because TAFs are a major focus for targeted cancer therapy, where their origin and specific characteristics are being targeted.

Acknowledgments We acknowledge the research and technical support from the School of Biomedical Sciences and Curtin Health Innovation Research Institute, Curtin University, where the work was carried out.

Authors' Contributions MV conceptualised, performed all experiments, analysed data, and drafted the manuscript. KK assisted the experiments performed using Seahorse flux analyser, its data analysis, interpretation and critical revision of the manuscript. FA was involved with conceptualisation and critical revision of manuscript. RD, PN were involved with critical revision of the manuscript. AD was involved with conceptualisation, critical revision of the manuscript, and funding of the experiments. All authors have read and approved the final version of this manuscript.

Funding MV is supported by scholarship from the Office of Research and Development, Faculty of Health sciences, Curtin University. MV would also like to acknowledge the contribution of an Australian Government Research Training Program Scholarship in supporting this research. AD is supported by strategic research funds from the School of Biomedical Sciences (Curtin University), Commercialisation Advisory Board of Curtin University, Cancer Council of Western Australia, and Actinogen Ltd., Perth, Western Australia.

Compliance with Ethical Standards

Not applicable.

Conflict of Interest The authors declare that they have no conflicts of interest.

Consent for Publication Not applicable.

Abbreviations ADSCs, Adipose-derived mesenchymal stem cells; TAFs, Tumour-associated fibroblasts; sFRP4, Secreted frizzled-related protein 4; TCM, Tumour conditioned medium; TGF-β, Transforming growth factor-beta; LPA, Lysophosphatidic acid; ECAR, Extracellular acidification rates; OCR, Oxygen consumption rates; DAPI, 4′,6-Diamidino-2-phenylindole dihydrochloride

References

1. Junttila MR, de Sauvage FJ (2013) Influence of tumour microenvironment heterogeneity on therapeutic response. Nature 501(7467):346–354. https://doi.org/10.1038/nature12626
2. Jotzu C, Alt E, Welte G, Li J, Hennessy BT, Devarajan E, Krishnappa S, Pinilla S, Droll L, Song YH (2011) Adipose tissue derived stem cells differentiate into carcinoma-associated fibroblast-like cells under the influence of tumor derived factors. Cell Oncol 34(1):55–67
3. Cho JA, Park H, Lim EH, Lee KW (2012) Exosomes from breast cancer cells can convert adipose tissue-derived mesenchymal stem cells into myofibroblast-like cells Int J Oncol:40
4. Cho JA, Park H, Lim EH, Kim KH, Choi JS, Lee JH (2011) Exosomes from ovarian cancer cells induce adipose tissue-derived mesenchymal stem cells to acquire the physical and functional characteristics of tumor-supporting myofibroblasts. Gynecol Oncol 123:379–386. https://doi.org/10.1016/j.ygyno.2011.08.005
5. Spaeth EL, Dembinski JL, Sasser AK, Watson K, Klopp A, Hall B, Andreeff M, Marini F (2009) Mesenchymal stem cell transition to tumor-associated fibroblasts contributes to fibrovascular network expansion and tumor progression. PLoS One 4(4):7
6. Mishra P, Humeniuk R, Medina D, Alexe G, Mesirov J, Ganesan S, Glod J, Banerjee D (2008) Carcinoma-associated fibroblast-like differentiation of human mesenchymal stem cells. Cancer Res 11: 4331–4339
7. Paunescu V, Bojin FM, Tatu CA, Gavriliuc OI, Rosca A, Gruia AT (2011) Tumour-associated fibroblasts and mesenchymal stem cells: more similarities than differences. J Cell Mol Med 15:635–646. https://doi.org/10.1111/j.1582-4934.2010.01044.x
8. Matushansky I, Hernando E, Socci ND, Mills JE, Matos TA, Edgar MA, Singer S, Maki RG, Cordon-Cardo C (2007) Derivation of sarcomas from mesenchymal stem cells via inactivation of the Wnt pathway. J Clin Invest 117(11):3248–3257
9. Jian H, Shen X, Liu I, Semenov M, He X, Wang XF (2006) Smad3-dependent nuclear translocation of beta-catenin is required for TGF-beta1-induced proliferation of bone marrow-derived adult human mesenchymal stem cells. Genes Dev 20(6):666–674. https://doi.org/10.1101/gad.1388806
10. Sato M (2006) Upregulation of the Wnt/beta-catenin pathway induced by transforming growth factor-beta in hypertrophic scars and keloids. Acta Derm Venereol 86(4):300–307. https://doi.org/10.2340/00015555-0101
11. DiRenzo DM, Chaudhary MA, Shi X, Franco SR, Zent J, Wang K, Guo L-W, Kent KC (2016) A crosstalk between TGF-β/Smad3 and Wnt/β-catenin pathways promotes vascular smooth muscle cell proliferation. Cell Signal 28(5):498–505. https://doi.org/10.1016/j.cellsig.2016.02.011
12. Zhou S (2011) TGF-β regulates β-catenin signaling and osteoblast differentiation in human mesenchymal stem cells. J Cell Biochem 112(6):1651–1660. https://doi.org/10.1002/jcb.23079
13. Akhmetshina A, Palumbo K, Dees C, Bergmann C, Venalis P, Zerr P, Horn A, Kireva T, Beyer C, Zwerina J, Schneider H, Sadowski A, Riener M-O, MacDougald OA, Distler O, Schett G, Distler JHW (2012) Activation of canonical Wnt signalling is required for TGF-β-mediated fibrosis. Nat Commun 3:735. https://doi.org/10.1038/ncomms1734
14. Saran U, Arfuso F, Zeps N, Dharmarajan A (2012) Secreted frizzled-related protein 4 expression is positively associated with responsiveness to cisplatin of ovarian cancer cell lines in vitro and with lower tumour grade in mucinous ovarian cancers. BMC Cell Biol 13(1):25
15. Muley A, Majumder S, Kolluru GK, Parkinson S, Viola H, Hool L, Arfuso F, Ganss R, Dharmarajan A, Chatterjee S (2010) Secreted

frizzled-related protein 4: an angiogenesis inhibitor. Am J Pathol 176(3):1505–1516
16. Wolf V, Ke G, Dharmarajan AM, Bielke W, Artuso L, Saurer S, Friis R (1997) DDC-4, an apoptosis-associated gene, is a secreted frizzled relative. FEBS Letters 417 (3):385–389. doi:doi:https://doi.org/10.1016/S0014-5793(97)01324-0
17. Warrier S, Balu SK, Kumar AP, Millward M, Dharmarajan A (2013) Wnt antagonist, secreted frizzled-related protein 4 (sFRP4), increases chemotherapeutic response of glioma stem-like cells. Oncol Res 21(2):93–102. https://doi.org/10.3727/096504013x13786659070154
18. Perumal V, Pohl S, Keane KN, Arfuso F, Newsholme P, Fox S, Dharmarajan A (2016) Therapeutic approach to target mesothelioma cancer cells using the Wnt antagonist, secreted frizzled-related protein 4: metabolic state of cancer cells. Exp Cell Res 341(2):218–224. https://doi.org/10.1016/j.yexcr.2016.02.008
19. Anderberg C, Pietras K (2009) On the origin of cancer-associated fibroblasts. Cell Cycle 8(10):1461–1462. https://doi.org/10.4161/cc.8.10.8560
20. Hanley CJ, Noble F, Ward M, Bullock M, Drifka C, Mellone M, Manousopoulou A, Johnston HE, Hayden A, Thirdborough S, Liu Y, Smith DM, Mellows T, Kao WJ, Garbis SD, Mirnezami A, Underwood TJ, Eliceiri KW, Thomas GJ (2016) A subset of myofibroblastic cancer-associated fibroblasts regulate collagen fiber elongation, which is prognostic in multiple cancers. Oncotarget 7 (5):6159–6174. doi:https://doi.org/10.18632/oncotarget.6740
21. Luo H, Tu G, Liu Z, Liu M (2015) Cancer-associated fibroblasts: a multifaceted driver of breast cancer progression. Cancer Lett 361(2):155–163. https://doi.org/10.1016/j.canlet.2015.02.018
22. Subramaniam KS, Tham ST, Mohamed Z, Woo YL, Mat Adenan NA, Chung I (2013) Cancer-associated fibroblasts promote proliferation of endometrial cancer cells. PLoS One 8(7):e68923. https://doi.org/10.1371/journal.pone.0068923
23. Tyan SW, Kuo WH, Huang CK, Pan CC, Shew JY, Chang KJ, Lee EY, Lee WH (2011) Breast cancer cells induce cancer-associated fibroblasts to secrete hepatocyte growth factor to enhance breast tumorigenesis. PLoS One 6(1):e15313. https://doi.org/10.1371/journal.pone.0015313
24. Noma K, Smalley KS, Lioni M, Naomoto Y, Tanaka N, El-Deiry W, King AJ, Nakagawa H, Herlyn M (2008) The essential role of fibroblasts in esophageal squamous cell carcinoma-induced angiogenesis. Gastroenterology 134(7):1981–1993. https://doi.org/10.1053/j.gastro.2008.02.061
25. Kellermann MG, Sobral LM, da Silva SD, Zecchin KG, Graner E, Lopes MA, Kowalski LP, Coletta RD (2008) Mutual paracrine effects of oral squamous cell carcinoma cells and normal oral fibroblasts: induction of fibroblast to myofibroblast transdifferentiation and modulation of tumor cell proliferation. Oral Oncol 44(5):509–517. https://doi.org/10.1016/j.oraloncology.2007.07.001
26. Jeon ES, Lee IH, Heo SC, Shin SH, Choi YJ, Park JH, Park DY, Kim JH (2010) Mesenchymal stem cells stimulate angiogenesis in a murine xenograft model of A549 human adenocarcinoma through an LPA1 receptor-dependent mechanism. Biochim Biophys Acta 1801(11):1205–1213. https://doi.org/10.1016/j.bbalip.2010.08.003
27. Gabbiani G, Ryan GB, Majne G (1971) Presence of modified fibroblasts in granulation tissue and their possible role in wound contraction. Experientia 27(5):549–550
28. Katoh K, Kano Y, Masuda M, Onishi H, Fujiwara K (1998) Isolation and contraction of the stress Fiber. Mol Biol Cell 9(7):1919–1938
29. Ronnov-Jessen L, Petersen OW (1993) Induction of alpha-smooth muscle actin by transforming growth factor-beta 1 in quiescent human breast gland fibroblasts. Implications for myofibroblast generation in breast neoplasia. Laboratory investigation; a journal of technical methods and pathology 68(6):696–707
30. Jeon ES, Moon HJ, Lee MJ, Song HY, Kim YM, Cho M, Suh DS, Yoon MS, Chang CL, Jung JS, Kim JH (2008) Cancer-derived lysophosphatidic acid stimulates differentiation of human mesenchymal stem cells to myofibroblast-like cells. Stem Cells 26(3):789–797. https://doi.org/10.1634/stemcells.2007-0742
31. Mazzocca A, Dituri F, Lupo L, Quaranta M, Antonaci S, Giannelli G (2011) Tumor-secreted lysophostatidic acid accelerates hepatocellular carcinoma progression by promoting differentiation of peritumoral fibroblasts in myofibroblasts. Hepatology 54(3):920–930. https://doi.org/10.1002/hep.24485
32. Gottschling S, Granzow M, Kuner R, Jauch A, Herpel E, Xu EC (2013) Mesenchymal stem cells in non-small cell lung cancer–different from others? Insights from comparative molecular and functional analyses Lung Cancer 80:19–29. https://doi.org/10.1016/j.lungcan.2012.12.015
33. Xu X, Zhang X, Wang S, Qian H, Zhu W, Cao H (2011) Isolation and comparison of mesenchymal stem-like cells from human gastric cancer and adjacent non-cancerous tissues. J Cancer Res Clin Oncol 137:495–504. https://doi.org/10.1007/s00432-010-0908-6
34. Ding G, Shao J, Ding Q, Fang Z, Wu Z, Xu J (2012) Comparison of the characteristics of mesenchymal stem cells obtained from prostate tumors and from bone marrow cultured in conditioned medium Exp Ther Med:4
35. Xu X, Zhang X, Wang S, Qian H, Zhu W, Cao H, Wang M, Chen Y, Xu W (2011) Isolation and comparison of mesenchymal stem-like cells from human gastric cancer and adjacent non-cancerous tissues. J Cancer Res Clin Oncol 137(3):495–504. https://doi.org/10.1007/s00432-010-0908-6
36. Lacher MD, Siegenthaler A, Jager R, Yan X, Hett S, Xuan L, Saurer S, Lareu RR, Dharmarajan AM, Friis R (2003) Role of DDC-4//sFRP-4, a secreted frizzled-related protein, at the onset of apoptosis in mammary involution. Cell Death Differ 10(5):528–538
37. Drake JM, Friis RR, Dharmarajan AM (2003) The role of sFRP4, a secreted frizzled-related protein, in ovulation. Apoptosis 8(4):389–397
38. Hinz B, Celetta G, Tomasek JJ, Gabbiani G, Chaponnier C (2001) Alpha-smooth muscle actin expression upregulates fibroblast contractile activity. Mol Biol Cell 12(9):2730–2741
39. Mar PK, Roy P, Yin HL, Cavanagh HD, Jester JV (2001) Stress Fiber Formation is Required for Matrix Reorganization in a Corneal Myofibroblast Cell Line. Experimental Eye Research 72 (4):455–466. doi:doi:https://doi.org/10.1006/exer.2000.0967
40. Ford CE, Jary E, Ma SS, Nixdorf S, Heinzelmann-Schwarz VA, Ward RL (2013) The Wnt gatekeeper SFRP4 modulates EMT, cell migration and downstream Wnt signalling in serous ovarian cancer cells. PLoS One 8(1):e54362. https://doi.org/10.1371/journal.pone.0054362
41. Bhuvanalakshmi G, Arfuso F, Millward M, Dharmarajan A, Warrier S (2015) Secreted frizzled-related protein 4 inhibits glioma stem-like cells by reversing epithelial to mesenchymal transition, inducing apoptosis and decreasing cancer stem cell properties. PLoS One 10(6):e0127517. https://doi.org/10.1371/journal.pone.0127517
42. Warburg O (1956) On the origin of cancer cells. Science 123(3191):309–314
43. Sotgia F, Martinez-Outschoorn UE, Pavlides S, Howell A, Pestell RG, Lisanti MP (2011) Understanding the Warburg effect and the prognostic value of stromal caveolin-1 as a marker of a lethal tumor microenvironment. Breast cancer research: BCR 13(4):213–213. https://doi.org/10.1186/bcr2892
44. Martinez-Outschoorn UE, Sotgia F, Lisanti MP (2012) Power surge: supporting cells "fuel" cancer cell mitochondria. Cell Metab 15(1):4–5. https://doi.org/10.1016/j.cmet.2011.12.011
45. Guido C, Whitaker-Menezes D, Capparelli C, Balliet R, Lin Z, Pestell RG, Howell A, Aquila S, Ando S, Martinez-Outschoorn U, Sotgia F, Lisanti MP (2012) Metabolic reprogramming of

cancer-associated fibroblasts by TGF-beta drives tumor growth: connecting TGF-beta signaling with "Warburg-like" cancer metabolism and L-lactate production. Cell Cycle 11(16):3019–3035. https://doi.org/10.4161/cc.21384

46. Zhang D, Wang Y, Shi Z, Liu J, Sun P, Hou X, Zhang J, Zhao S, Zhou BP, Mi J (2015) Metabolic reprogramming of cancer-associated fibroblasts by IDH3alpha downregulation. Cell Rep 10(8):1335–1348. https://doi.org/10.1016/j.celrep.2015.02.006
47. G B AF, Millward M, Dharmarajan A, Warrier S (2015) Secreted frizzled-related protein 4 inhibits glioma stem-like cells by reversing epithelial to mesenchymal transition, inducing apoptosis and decreasing Cancer stem cell properties. PLoS One 10(6): e0127517. https://doi.org/10.1371/journal.pone.0127517